第 35 卷第 12 期
2019 年 12 月

无 机 化 学 学 报
CHINESE JOURNAL OF INORGANIC CHEMISTRY

Vol.35 No.12
2337-2345

锌卟啉自组装在染料敏化太阳能电池中的应用

贾海浪* 彭智杰 李珊珊 龚炳泉 关明云
(江苏理工学院化学与环境工程学院,常州 213001)

摘要:制备了 2 种锌卟啉天线分子 P2 与 P3,并通过自组装的方法成功地将这些天线分子应用到了染料敏化太阳能电池之中。与传统的 D-π-A 结构的染料相比,这种策略显示出了明显的优势:可以避免复杂的合成步骤,还可以通过调节天线分子和锚固基团的结构去改善染料的光子捕获能力并减少电荷复合行为。当 4-吡啶-4-基苯甲酸(A)作为锚固基团时,经过分子自组装之后,基于 A-P2 的电池器件显示出了 1.68%的转换效率,开路电压为 526 mV,短路电流密度为 5.39 mA·cm^{-2},这充分说明了自组装策略在染料敏化太阳能电池中得到了很好的应用。而基于 A-P3 的电池器件能量转换效率只有 0.79%,这可能主要是因为天线分子 P3 较大的位阻减小了染料吸附量的原因造成的。我们另外也测试比较了它们在光学、电化学、光伏性能等方面的差异。

关键词:染料敏化太阳能电池;锌卟啉;自组装;天线分子
中图分类号:O614.24+1 **文献标识码**:A **文章编号**:1001-4861(2019)12-2337-09
DOI:10.11862/CJIC.2019.274

Self-Assembly with Zinc Porphyrin Antenna for Dye-Sensitized Solar Cells

JIA Hai-Lang* PENG Zhi-Jie LI Shan-Shan GONG Bing-Quan GUAN Ming-Yun
(*School of Chemical and Environmental Engineering, Jiangsu University of Technology, Changzhou* 213001, *China*)

Abstract: Two antenna molecules zinc porphyrin P2, P3 were prepared, and these antenna molecules have been successfully used in DSSCs (dye-sensitized solar cells) through supramolecular self-assembly. Compared with traditional D-π-A structure dyes, this strategy shows obvious advantages. This method can avoid complex synthesis steps, the light-harvesting ability of dyes can be improved and charge recombination can be reduced by adjusting the antenna molecules and anchoring groups. When 4-pyrid-4-ylbenzoic acid (A) was used as the anchoring group, after supramolecular self-assembly, the device of A-P2 displayed a PCE (power conversion efficiency) of 1.68%, and the V_{oc} was 526 mV, the J_{sc} was 5.39 mA·cm^{-2}. This indicates that the supramolecular self-assembly strategy has been successfully applied in DSSC. The device of A-P3 displayed the PCE of 0.79%, which is mainly due to the lower amount of dye loading. In addition, the optical properties, electrochemical properties, photovoltaic performance were also studied.

Keywords: dye-sensitized solar cells; zinc porphyrin; self-assembly; antenna molecule

0 Introduction

In recent years, the rapid development of economy has also brought about serious environmental pollution and energy shortage, and people show more and more interest in the development and utilization of new energy. New energy has incomparable advantages compared with traditional energy, such as abundant sources, easy development, environmental friendliness, recycling and so on. Among them, solar

收稿日期:2019-04-25。收修改稿日期:2019-09-18。
国家自然科学基金(No.21701060)、常州科技计划(No.CJ20190079)、江苏省教育厅项目(No.17KJB150015,18KJA150003)。
*通信联系人。E-mail:jiahailang85@126.com

energy has great application potential, it has become one of the important areas of new energy[1-2]. Many researchers are devoted to the research of DSSCs (dye-sensitized solar cells), the DSSCs have many advantages compared with traditional energy, such as low cost, simple fabrication process, wide source of raw materials, multi-color transparency, high photoelectric conversion efficiency and environmental friendliness[3-5]. After more than 20 years of development, DSSCs have made great progress, up to now, the device of ADEKA-1 exhibited the highest PCE of 14.3%[6].

Dyes play an important role in DSSCs, due to TiO_2 is a wide band material, it can only absorb ultraviolet rays and the utilization of sunlight is very low, on the contrary, dyes can broaden the absorption of DSSCs to visible and even near infrared regions[7-8]. So far, many research groups have designed and synthesized many new dyes. Generally speaking, ideal dyes need to meet the following conditions: (1) dyes can absorb sunlight in visible and even infrared regions, (2) dyes contain carboxyl (-COOH), sulfonic acid ($-SO_3H$), phosphoric acid ($-PO_3H_2$), pyridine and other anchoring groups, (3) high quantum efficiency, (4) the excited state energy level of dyes should match the conduction level of TiO_2, (5) dyes should have high oxidation potential and high regeneration efficiency, (6) dyes have good stability and can be recycled 10^5 times[9-12]. So far, there are two kinds of efficient dyes for DSSCs, metal complexes and metal-free organic dyes[13-16]. Many excellent dyes have been prepared, the PCE of some of these dyes has exceeded 10%[17-20]. In 2005, ruthenium complex dye N719 was prepared, the PCE of N719 achieved 11.18%[21]. In 2010, Wang prepared ruthenium complex C106, the value of PCE was up to 11.7%[22]. In addition, many metalloporphyrin dyes have excellent photoelectric properties, Grätzel and co-workers reported an excellent porphyrin dye YD2-o-C8, the PCE of the device reached 12.3%[23-27]. In 2014, Grätzel and co-workers synthesized a more efficient dye SM315, under the condition of using cobalt-based redox electrolyte, the PCE of the device was up to 13%[28]. Organic dyes have also developed rapidly, these dyes have good application prospects, which has obvious advantages compared with metal complexes, such as easy modification, low price, good plasticity and easy degradation[29-32]. Some excellent dyes have been successfully prepared, such as C275, DTS-CA, HL7[33-35].

Nevertheless, this is still far from the theoretical efficiency (33%), how to achieve higher PCE on the basis of the previous is a major challenge for DSSCs. Many dyes require complex synthetic steps, which have been troubling researchers, in addition, the monolayer structure of dye molecules always restricts the development of DSSCs, thus, we need to develop some new structures and methods. Construction of multilayer dyes by supramolecular self-assembly strategy may be a promising way to improve the performance of DSSCs. The method is easy to operate, by adjusting the antenna molecules and anchoring groups, the light-harvesting ability of dyes can be improved and charge recombination can be reduced, and complex synthesis is not required[36-38]. What's more, the amount of dye adsorbed will not decrease, this may change the limitation of monolayer dyes of DSSCs. Saha and co-workers used ZnPc and PyPMI as antenna molecules and anchoring groups, respectively, after supramolecular self-assembly, the PCE of PyPMI-ZnPc was 3 times than that of device of PyPMI[39].

Hererin, we prepared two antenna molecules zinc porphyrin P2 and P3. The zinc porphyrin was choosed as antenna molecule due to its excellent photoelectric properties, which has good absorption in a range of 400~450 nm (Soret band) and 500~700 nm (Q band), this will be very helpful to improve the light-harvesting ability of devices. 4-Pyrid-4-ylbenzoic acid (A) was used as the anchoring group, which can coordinate with zinc porphyrin, after supramolecular self-assembly, the DSSCs based on A-P show obvious photovoltaic performance. The device of A-P2 exhibited the PCE of 1.68%, and the V_{oc} is 526 mV, the J_{sc} is 5.39 mA·cm^{-2}, which is better than that of A-P3. We also studied the optical properties, electrochemical properties, photovoltaic performance to analyze the differences between them.

1 Experimental

1.1 Synthesis

The structures of P2, P3 were shown in Fig.1, and the synthesis method of the two antenna molecules was shown in Fig.2. All solvents were treated by standard methods before use and all chemicals were purchased from commercial suppliers and used without further purification unless indicated otherwise. The ^{1}H NMR were recorded on a Bruker DRX NMR spectrometer with tetramethylsilane (TMS) as the internal standard.

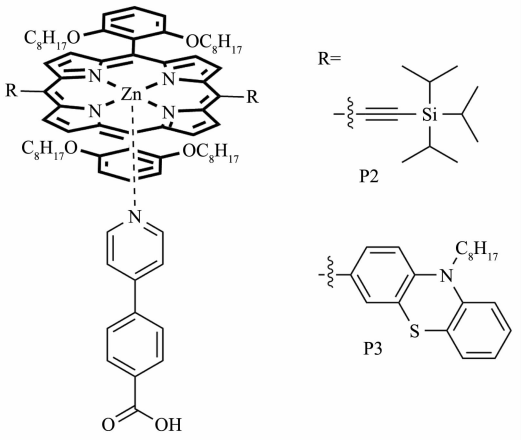

Fig.1　Self-assembly of A (4-pyrid-4-ylbenzoic acid) with P2 or P3

1.1.1　Synthesis of compound **2**

The compound **1** (2.00 g, 2.05 mmol) was were dissolved in DCM (500 mL), then the temperature is cooled to 0 ℃, and the NBS (0.75 g, 4.20 mmol, in 30 mL DCM) was dropped slowly. After 6 h, the mixture was quenched with acetone, and evaporated *in vacuo*. Then the residue was dissolved in DCM (200 mL) and MeOH (100 mL), the $Zn(OAc)_2\cdot 2H_2O$ (2.25 g, 10.25 mmol) was added, the mixture was stirred at room temperature for 2 h. The mixture was washed with brine, dried over $MgSO_4$, and evaporated *in vacuo*. The residue was purified by silica gel column chromatography (V_{PE}:V_{EA}=10:1) to give compound **2** (1.83 g, 75%). ^{1}H NMR ($CDCl_3$, 500 MHz): δ_H 9.66~9.67 (m, 4H), 8.92~8.95 (m, 4H), 7.72 (t, *J*=8.5 Hz, 2H), 7.02 (d, *J*=8.5 Hz, 4H), 3.86 (t, *J*=6.0 Hz, 8H), 0.96~0.99 (m, 8H), 0.80~0.84 (m, 8H). 0.38~0.63 (m, 44H).

1.1.2　Synthesis of P2

A mixture of compound **2** (1.00 g, 0.84 mmol), triisopropylacetylene (0.46 g, 2.51 mmol), CuI (32 mg, 0.17 mmol) in THF (60 mL) and Et_3N (10 mL). Then the $Pd(PPh_3)_2Cl_2$ (0.20 g) was added under N_2, the mixture was heated under 80 ℃ for overnight. The

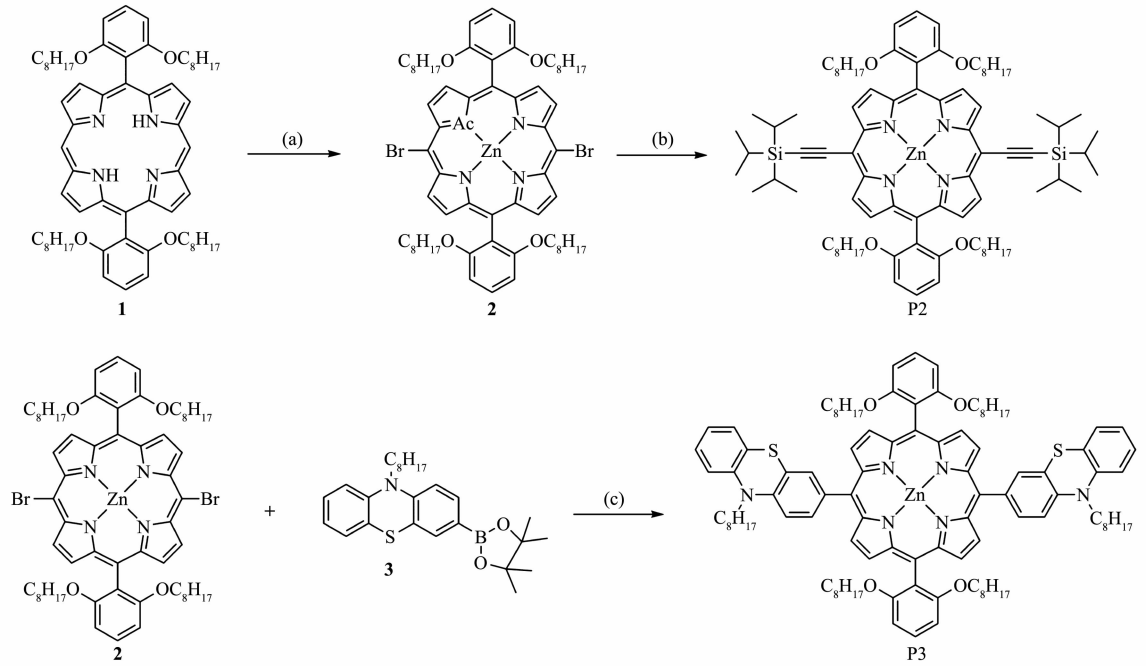

Reagents and conditions: (a) NBS, $Zn(OAc)_2\cdot 2H_2O$, (b) triisopropylacetylene, $Pd(PPh_3)_2Cl_2$, CuI, THF, Et_3N, (c) $Pd(PPh_3)_4$, K_2CO_3, H_2O

Fig.2　Synthesis procedure of P2 and P3

reaction mixture was cooled to room temperature and evaporated *in vacuo*. The residue was purified by silica gel column chromatography (V_{DCM}:V_{PE}=1:4) to give P2 (0.71 g, 61%). ^{1}H NMR ($CDCl_3$, 500 MHz): δ_H 9.66 (d, *J*=4.5Hz, 4H), 8.87 (d, *J*=4.5 Hz, 4H), 7.69 (t, *J*=8.5 Hz, 2H), 7.00 (d, *J*=6.0Hz 4H), 3.85 (t, *J*=6.0 Hz, 8H), 1.45~1.51 (m, 42H), 0.92~0.98 (m, 8H), 0.80 ~0.84 (m, 8H). 0.39~0.63 (m, 44H).

1.1.3 Synthesis of P3

Under nitrogen, compound **2** (100 mg, 84 μmol), compound **3** (110 mg, 250 μmol), K_2CO_3 (46 mg, 334 μmol) and $Pd(PPh_3)_4$ (30 mg) were dissolved in 1,4-dioxane (30 mL) and H_2O (5 mL). The mixture was heated under 90 ℃ for overnight. The reaction mixture was cooled to room temperature and extracted by DCM (3×30 mL). The combined organic layers were washed with brine, dried over $MgSO_4$, and evaporated *in vacuo*. The residue was purified by silica gel column chromatography (V_{DCM}:V_{PE}=1:4) to give P3 (101 mg, 73%). ^{1}H NMR ($CDCl_3$, 400 MHz): δ_H 8.76~8.83 (m, 8H), 7.93~7.97 (m, 4H), 7.64~7.68 (m, 2H), 7.22 ~7.28 (m, 3H), 7.16 (d, *J*=8.4 Hz, 2H), 6.96~7.04 (m, 9H), 4.08 (t, *J*=7.2 Hz, 4H), 3.80 (t, *J*=6.4 Hz, 8H), 2.01 ~2.08 (m, 4H), 1.55~1.63 (m, 4H), 1.26~1.47 (m, 16H), 0.83~0.97 (m, 24H), 0.68~0.73 (m, 8H), 0.45~0.59 (m, 34H).

1.2 Fabrication of DSSCs

The working electrode (active area is 0.196 cm^2) was prepared by screen printing the TiO_2 paste on Fluorine-doped tin oxide (FTO) glass plates (15 $\Omega \cdot m^{-2}$). For preparation of a DSSC, FTO glass plates were cleaned in a detergent solution using an ultrasonic bath for 30 min for two times and then rinsed with water and ethanol. Then, the plates were immersed into 40 mmol·L^{-1} $TiCl_4$ (aqueous) at 70 ℃ for 30 min and washed with water and ethanol. The TiO_2 paste consisted of 12 μm thick film (particle size, 20 nm, pore size 32 nm). The TiO_2 films were performed with a programmed procedure: (1) 80 ℃ for 15 min; (2) 135 ℃ for 10 min; (3) 325 ℃ for 30 min; (4) 375 ℃ for 5 min; (5) 450 ℃ for 15 min, and (6) 500 ℃ for 15 min. Then the films were treated again with $TiCl_4$ at 70 ℃ for 30 min and sintered at 500 ℃ for 30 min. Then the electrode was immersed into 2 mmol·L^{-1} A solution (methanol) for 2 h at room temperature, then rinsed with ethanol, and then was immersed into 1 mmol·L^{-1} P solution (V_{THF}:V_{EtOH}=4:1) for 18 h to form supramolecules on the TiO_2 surface and dried in air. The working electrode and the Pt counter electrode were then sealed with a Surlyn film (25 μm) by heating the sandwich-type cell at 110 ℃. The electrolyte was introduced through pre-drilled holes in the counter electrode and was driven into the cell via vacuum backfilling, and the hole was sealed with a Surlyn film and a thin glass (0.1 mm thickness) cover by heating. The electrolyte was composed of 0.6 mol·L^{-1} 1-butyl-3-methylimidazolium iodide (BMII), 50 mmol·L^{-1} I_2, 50 mmol·L^{-1} LiI, 0.5 mol·L^{-1} *tert*-butylpyridine and 0.1 mol·L^{-1} guanidiniumthiocyanate (GuNCS) in acetonitrile.

1.3 Characterizations of DSSCs

The photocurrent-voltage (*I-V*) curves of the DSSCs were measured on a Keithley 2400 source meter under standard global AM 1.5G solar irradiation supplied by a xenon light source (Oriel). The incident photo-to-electron conversion efficiency (IPCE) spectra of the DSSCs were measured by a DC method. The light source was a 300 W xenon lamp (Oriel 6258) coupled with a flux controller to improve the stability of the irradiance. The single wavelength was selected by a monochromator (Cornerstone 260 Oriel74125). Light intensity was measured by a NREL traceable Si detector (Oriel 71030NS) and the short circuit currents of the DSSCs were measured by an optical power meter (Oriel 70310).

1.4 UV-Vis spectroscopy, electrochemical properties and amounts of dye loading

The UV-Vis absorption spectra were recorded on a Shimadzu UV-3600 spectrometer. The cyclic voltammograms (CV) of the dyes and electrochemical impedance spectroscopy (EIS) were studied using a Chenhua CHI760E model Electrochemical Workstation (Shanghai). The amounts of dye loading were estimated according to the following methods: the sensitized electrodes were immersed into a 0.1 mol·L^{-1} NaOH solution in a mixed solvent (V_{H_2O}:V_{THF}=1:4),

which resulted in desorption of each dye. The amounts of dye loading can be estimated according to the following formula: $C=AV/(\varepsilon S)$, where C stands for the amounts of dye loading, A is optical absorbance of the dye, V is volume of desorption solution, ε is molar extinction coefficients, S is effective area of TiO_2 films.

2 Results and discussion

2.1 Optical properties

As shown in Fig.3a, we measured the absorption spectra of P2 and P3 in DCM. It is obvious that all the antenna molecules show standard porphyrin absorption peaks, they have characteristic absorption in the range of 400~450 nm (Soret band) and 500~700 nm (Q band), the band of 400~700 nm can be attributed to electronic transitions from π-π* and intramolecular charge transfer (ICT). The antenna molecule porphyrin P2 displays high absorption coefficient (2.26×10^5 L·mol^{-1}·cm^{-1}) at 438 nm in Soret band, and medium absorption coefficient at 580 nm (8.20×10^3 L·mol^{-1}·cm^{-1}) and 631 nm (2.20×10^4 L·mol^{-1}·cm^{-1}), respectively. From this, we can see that antenna molecule P2 has good spectral response in visible region, this in favor of enhancing the light-harvesting capability of dyes, thereby increasing J_{sc} (short-circuit current density) of DSSCs. When the R group is replaced by phenothiazine, the absorption spectrum of P3 shows a slight hypsochromic-shift compared with P2, this may be due to the non-planar steric effect between porphyrin ring and phenothiazine. The antenna molecule porphyrin P3 displays high molar extinction coefficient (2.39×10^5 L·mol^{-1}·cm^{-1}) at 436 nm, with medium absorption coefficient at 567 nm (1.16×10^4 L·mol^{-1}·cm^{-1}) and 614 nm (1.12×10^4 L·mol^{-1}·cm^{-1}), respectively.

In order to study the changes of absorption spectra, we further measured the spectral response performance of the three supermolecules anchored on 12 μm TiO_2 films (Fig.3b). As shown in Fig.4, The TiO_2 film was first immersed into 2 mmol·L^{-1} A solution for 2 h at room temperature and rinsed with ethanol, then was immersed into 1 mmol·L^{-1} P solution to form supramolecules on the TiO_2 surface and dried in air. From Fig.3b, we can see that the absorption spectra have changed a lot compared with those of P2, P3 in DCM, the absorption spectra have been significantly improved, their absorption ranges all are over 650 nm, even up to 700 nm. This indicates that the light-harvesting ability of dyes has been improved greatly after supramolecular self-assembly, this will improve the J_{sc} of the DSSCs. From Fig.3a, we can see that there is little difference in spectral response between P2 and P3, after self-assembly, the absorption spectrum of A-P2 was obviously better than that of A-P3, we infer that this should be attributed mainly to the difference in the antenna molecules loading amounts. To better analyze the differences between their absorption spectra, the amounts of dye loading were further measured. After self-assembed with porphyrin chromophores, the value of loading amount of P2 is about 1.12×10^{-8} mol·cm^{-2}, and the value of

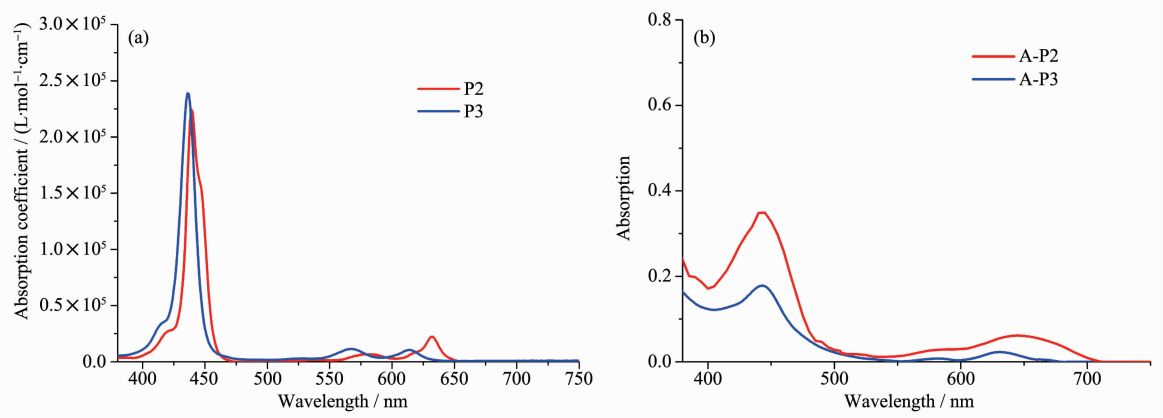

Fig.3 (a) UV-Vis absorption spectra of P1, P2 and P3 in DCM, (b) UV-Vis absorption spectra of A-P1, A-P2 and A-P3 anchored on TiO_2 surface

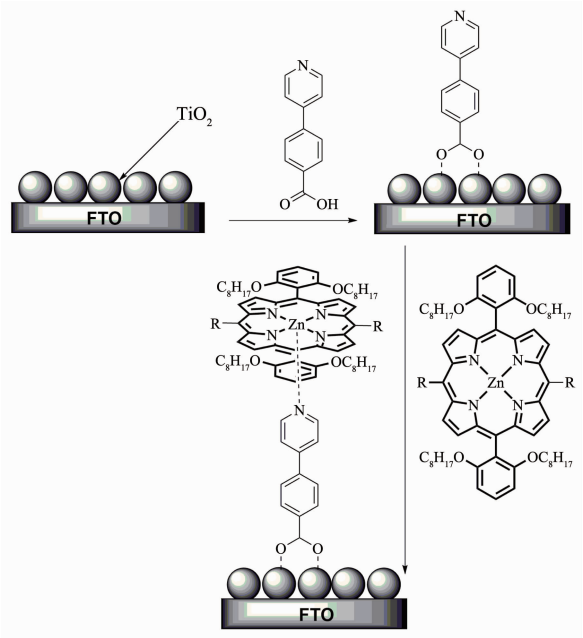

Fig.4 Schematic diagram of self-assembly

P3 is only about 0.51×10^{-8} mol·cm^{-2}, the largest loading amount of P2 can enhance the light-harvesting ability of the device well.

2.2 Electrochemical properties

In the process of dye design, the excited state energy level of dyes should match the conduction level of TiO_2, and dyes should have high oxidation potential and high regeneration efficiency[40-41]. In order to study the related properties, we measured the cyclic voltammetry curves of A-P2 and A-P3 anchored on TiO_2 (Fig.5). As shown in Fig.5, the E_{OX} (ground state oxidation potentials) of A-P2 and A-P3 were 0.93 and 0.79 V (versus NHE), respectively. As we known, the redox potential of the I^-/I_3^- is 0.4 V, while the E_{OX} of the two supramolecules all are much positive than 0.4 V, the result indicates that the oxidized dyes can be effectively recycled. We estimated the energy gap (E_{0-0}) by their absorption spectra, and the values of A-P2 and A-P3 are 1.77 and 1.82 eV, respectively. Thus, the excited oxidation potentials (E_{OX}*) of A-P2 and A-P3 are −0.84 and −1.03 V, respectively. They are all negative than the conduction band of TiO_2 (−0.5 V versus NHE), this indicates that the electron from the excited dyes of A-P2 and A-P3 all have high electron injection efficiency[42-43].

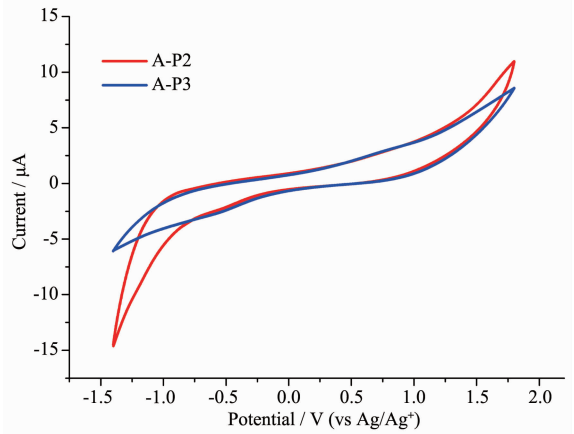

In DCM, 0.1 mol·L^{-1} $TBAPF_6$, photoanode as working electrode, Pt as counter electrode, Ag/Ag^+ as reference electrode, scan rate: 100 mV·s^{-1}, calibrated with ferrocene/ferrocenium (Fc/Fc^+) as an external reference

Fig.5 Cyclic voltammogram of A-P2 and A-P3

2.3 Photovoltaic performance of DSSCs

The photovoltaic performance of the devices based on supramolecular self-assembly were measured, the *J-V* (photocurrent-density-photovoltage) curves of the devices were measured (Fig.6), and Table 1 shows the related parameters. As designed, the antenna molecules P2, P3 can coordinate with the anchoring groups (A) to form supermolecules A-P2 and A-P3, after self-assembly, the DSSCs based on these supermolecules exhibit remarkable photovoltaic performance. The device of A-P2 shows the highest PCE of 1.68%, with a value of V_{oc} is 526 mV, a value of J_{sc} is 5.39 mA·cm^{-2}, and a value of FF is 59.20%. Compared with A-P2, the performance of A-P3 has slightly decreased, the PCE droped down to 0.79%. The main reason is that the V_{oc} decreased from 526 to 478 mV and the J_{sc} decreased from 5.39 mA·cm^{-2} to 3.02 mA·cm^{-2}. In addition, the loading amounts of P2, P3 have been measured, and the value of P2 (1.12×10^{-8} mol·cm^{-2}) is much higher than that of P3 (0.51×10^{-8} mol·cm^{-2}). We can see that the loading amount has a great influence on the performance of DSSCs, the highest loading amount of P2 can make up for the deficiency of spectral response, this will not only enhance the light-harvesting capability of devices, on the other hand, close alignment of antenna molecules may can effectively prevent the I_3^- penetrating into the TiO_2 surface, thus, the charge recombination can be reduced.

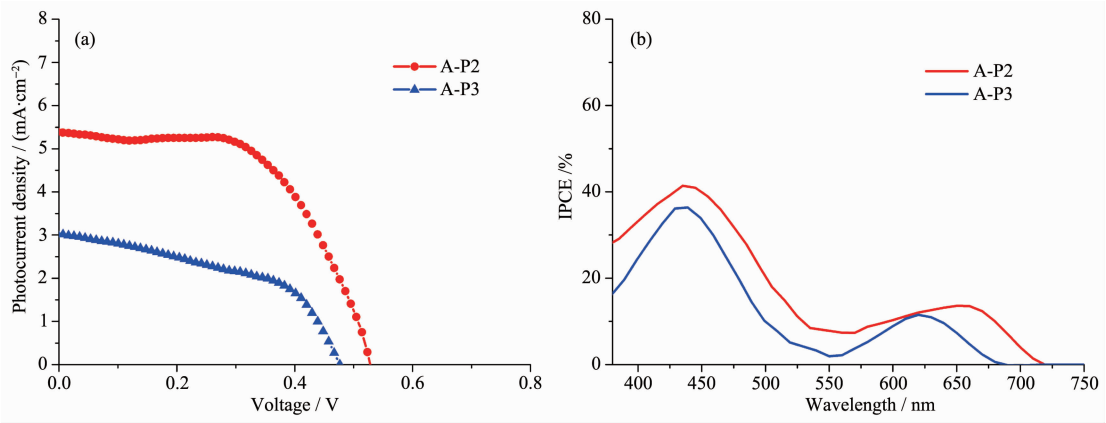

Fig.6　(a) *I-V* curves of A-P2 and A-P3, (b) IPCE curves of A-P2 and A-P3

Table 1　Photovoltaic parameters of the DSSCs obtained from the *J-V* curves

Dye	J_{sc} / (mA·cm^{-2})	V_{oc} / V	FF / %	η / %
A-P2	5.39±0.02	0.526±0.000	59.20±0.73	1.68±0.02
A-P3	3.02±0.01	0.478±0.001	54.48±0.40	0.79±0.00

Size of the active area for each cell is 0.196 cm^2, three devices are assembled in parallel with each dye, the DSSCs were all measured under standard global AM 1.5G solar irradiation.

We find that the J_{sc} of these DSSCs decreases in turn along the following trend: A-P2 (5.39 mA·cm^{-2}) > A-P3 (3.02 mA·cm^{-2}). The incident photon-to-current conversion efficiency (IPCE) spectra of the DSSCs were measured to analysis the differences. From Fig. 6b, the IPCE curves of A-P2 exhibited the highest value of 41.9% at 437 nm, and the photocurrent generation up to about 720 nm. The IPCE curves of A-P3 exhibited the photocurrent generation up to about 680 nm, the value at 434 nm was only 36.5%. In the long wave region, we also found that photocurrent of A-P2 was better than that of A-P3, this should be attributed to the larger loading amount of A-P2.

2.4　EIS measurements

Electrochemical Impedance Spectroscopy (EIS) is an important method for studying the charge transfer properties at the interface of DSSCs, in this work, we measured the EIS to analyze charge recombination dynamics under dark[44-47]. As we known, the charge recombination rate has an important influence on V_{oc}. The EIS was measured under the applied voltage of −0.6 V to analyze the difference between V_{oc}. From Fig.7, two semicircles were found in the plots, the small semicircle means the transport resistance at the Pt/electrolyte, and the large semicircle means the

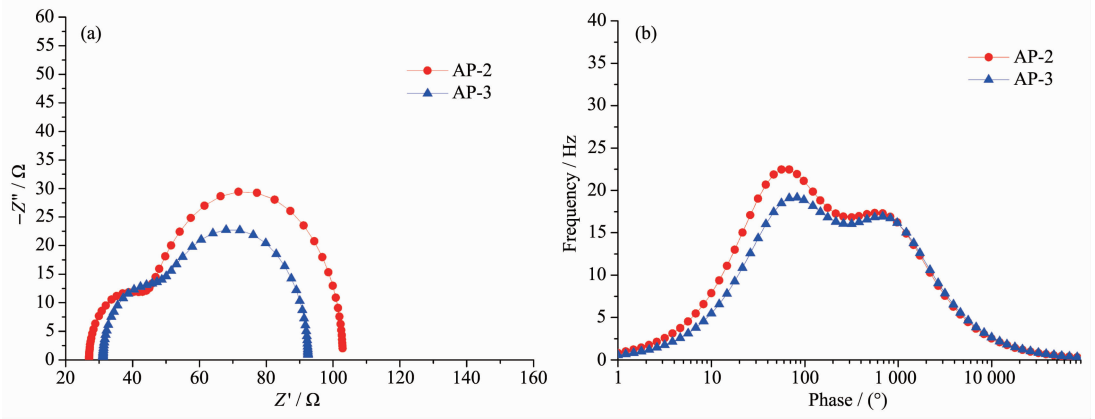

Fig.7　(a) Nyquist plots of A-P2 and A-P3, (b) Bode phase plots of DSSCs based on A-P2 and A-P3

charge transfer resistance at the TiO_2/dye/electrolyte interface. We can see that the radius of the large semicircle of A-P2 is larger than that of A-P3, this means that the device of A-P2 effectively reduces the electron recombination rate after self-assembly, it is conducive to suppressing dark current and improving V_{oc}, this also explains why V_{oc} of A-P2 has the largest value of 526 mV. In addition, the electron lifetimes of the DSSCs were further measured by bode phase plots. The DSSC with longer electron lifetime indicates that there will be low dark current for the device, this helps to enhance the V_{oc}. The peak frequency (f) at lower frequency region can be readed from Fig.7b, and the electron lifetime (τ) can be calculated by $\tau=1/(2\pi f)$[48-49]. The f of A-P2 and A-P3 are 63.2 and 76.5 Hz, respectively. As a result, the electron lifetime values of A-P2 and A-P3 are 2.51 and 2.08 ms, respectively. The trend is consistent with the V_{oc} of DSSCs.

3 Conclusions

In summary, we used a simple method to improve the performance of DSSCs, two antenna molecules zinc porphyrin P2, P3 were prepared and then self-assembly was carried out by coordination with anchoring group (A, 4-pyrid-4-ylbenzoic acid). This method shows obvious advantages, it can avoid complex synthesis steps and improve the light-harvesting ability of dyes and reduce charge recombination by adjusting the antenna molecules and anchoring groups. After supramolecular self-assembly, the device of A-P2 showed a PCE of 1.68%, and a V_{oc} of 526 mV, a J_{sc} of 5.39 mA·cm^{-2}, and a FF of 59.20%, in contrast, the device of A-P3 showed a PCE of 0.79%, the main reason should be that the different structures of antenna molecules lead to different loading amount. The results show that self-assembly strategy has been successfully used in this work, this will be a potential and effective way to improve the performance of DSSCs.

Acknowledgements: This work was supported by grants from the National Natural Science Foundation of China (21701060), Changzhou Sci Tech Program (CJ20190079), China and Natural Science Foundation of the Higher Education Institutions of Jiangsu Province (17KJB150015, 18KJA150003), China.

References:

[1] Ardo S, Meyer G J. *Chem. Soc. Rev.*, **2009**,**38**:115-164

[2] Wu J, Lan Z, Lin J, et al. *Chem. Rev.*, **2015**,**115**:2136-2173

[3] YANG Ying(杨英), PAN De-Qun(潘德群), GAO Jing(高菁), et al. *Chinese J. Inorg. Chem.*(无机化学学报), **2018**,**34**:615-626

[4] Hagfeldt A, Boschloo G, Sun L, et al. *Chem. Rev.*, **2010**, **110**:6595-6663

[5] Zhang Q, Uchaker E, Candelariaza S L, et al. *Chem. Soc. Rev.*, **2013**,**42**:3127-3171

[6] Kakiage K, Aoyama Y, Yano T, et al. *Chem. Commun.*, **2015**, **51**:15894-15897

[7] Ragoussi M E, Torres T. *Chem. Commun.*, **2015**,**51**:3957-3972

[8] Li C T, Wu F L, Lee B H, et al. *ACS Appl. Mater. Interfaces*, **2017**,**9**:43739-43746

[9] ZHOU Wei-Nan(周伟男), ZHAO Hong-Bin(赵鸿斌), CAI Zhuo-Di(蔡卓弟), et al. *Chinese J. Inorg. Chem.*(无机化学学报), **2016**,**32**:81-88

[10]Huang L, Ma P, Deng G, et al. *Dyes Pigm.*, **2018**,**159**:107-114

[11]Miao K, Liang M, Wang Z, et al. *Phys. Chem. Chem. Phys.*, **2017**,**19**:1927-1936

[12]Zeng K, Lu Y, Tang W, et al. *Chem. Sci.*, **2019**,**10**:2186-2192

[13]Lu J, Liu S, Wang M, et al. *Front. Chem.*, **2018**,**6**:541

[14]Boaretto R, Carli S, Caramori S, et al. *Dalton Trans.*, **2017**, **46**:16390-16393

[15]Patil D S, Sonigara K K, Jadhav M M, et al. *New J. Chem.*, **2018**,**42**:4361-4371

[16]Tang Y, Wang Y, Li X, et al. *ACS Appl. Mater. Interfaces*, **2015**,**7**:27976-27985

[17]Cheng Y, Yang G, Jiang H, et al. *ACS Appl. Mater. Interfaces*, **2018**,**10**:38880-38891

[18]Song H, Liu Q, Xie Y, et al. *Chem. Commun.*, **2018**,**54**:1811-1824

[19]Yun S, Qin Y, Uhl A R, et al. *Energy Environ. Sci.*, **2018**, **11**:476-526

[20]Yang L, Chen S, Zhang J, et al. *J. Mater. Chem. A*, **2017**,**5**: 3514-3522

[21]Nazeeruddin M K, Angelis F D, Fantacci S, et al. *J. Am. Chem. Soc.*, **2005**,**127**:16835-16847

[22]Yu Q J, Wang Y H, Yi Z H, et al. *Acs, Nano.*, **2010**,**4**:6032-6038

[23]Wang C L, Zhang M, Hsiao Y H, et al. *Energy Environ. Sci.*, **2016**,**9**:200-206

[24]Krishna J V S, Krishna N V, Chowdhury T H, et al. *J. Mater. Chem.* C, **2018**,**6**:11444-11456

[25]Song H, Zhang J, Jin J, et al. *J. Mater. Chem. C*, **2018**,**6**:3927-3936

[26]Ji J M, Zhou H, Kim H K, et al. *J. Mater. Chem. A*, **2018**,**6**:14518-14545

[27]Yella, Lee H W, Tsao H N, et al. *Science*, **2011**,**334**:629-634

[28]Mathew S, Yella A, Gao P, et al. *Nat. Chem.*, **2014**,**6**:242-247

[29]Pei K, Wu Y, Li H, et al. *ACS Appl. Mater. Interfaces*, **2015**, **7**:5296-5304

[30]Qian X, Zhu Y Z, Chang W Y, et al. *ACS Appl. Mater. Interfaces*, **2015**,**7**:9015-9022

[31]Han M L, Zhu Y Z, Liu S, et al. *J. Power Sources*, **2018**, **387**:117-125

[32]Mao M, Li Q S, Zhang X L, et al. *Dyes Pigm.*, **2017**,**141**:148-160

[33]Yao Z, Wu H, Li Y, et al. *Energy Environ. Sci.*, **2015**,**8**:3192-3197

[34]Hung W I, Liao Y Y, Lee T H, et al. *Chem. Commun.*, **2015**, **51**:2152-2155

[35]Jradi F M, Kang X, O′Neil D, et al. *Chem. Mater.*, **2015**,**27**:2480-2487

[36]Subbaiyan N K, Hill J P, Ariga K, et al. *Chem. Commun.*, **2011**,**47**:6003-6005

[37]Nogueira A F, Furtado L F O, Formiga A L B, et al. *Inorg. Chem.*, **2004**,**43**:396-398

[38]Han F M, Yang J Y, Zhe Y, et al. *Dalton Trans.*, **2016**,**45**:8862-8868

[39]Panda D K, Goodson F S, Ray S, et al. *Chem. Commun.*, **2014**,**50**:5358-5360

[40]Zhao D X, Bian L Y, Luo Y X, et al. *Dyes Pigm.*, **2017**,**140**:278-285

[41]Zhang L Y, Zou S J, Sun X H, et al. *RSC Adv.*, **2018**,**8**:6212-6217

[42]Krishna N V, Krishna J V S, Singh S P, et al. *J. Phys. Chem. C*, **2017**,**121**:25691-25704

[43]Li C T, Wu F L, Lee B H. *ACS Appl. Mater. Interfaces*, **2017**,**9**:43739-43746

[44]Wu J, Li G, Zhang L, et al. *J. Mater. Chem. A*, **2016**,**4**:3342-3355

[45]Chen Y F, Liu J M, Huang J F, et al. *J. Mater. Chem. A*, **2015**,**3**:8083-8090

[46]Desta M B, Vinh N S, Kumar C P, et al. *J. Mater. Chem. A*, **2018**,**6**:13778-13789

[47]Li W, Wu Y, Zhang Q, et al. *ACS Appl. Mater. Interfaces*, **2012**,**4**:1822-1830

[48]Babu D D, Su R, El-Shafei A, et al. *RSC Adv.*, **2016**,**6**:30205-30216

[49]Yen Y S, Ni J S, Hung W I, et al. *ACS Appl. Mater. Interfaces*, **2016**,**8**:6117-6126